Reduced length buckling restrained brace using steel plates as restraining segment

S.A. Razavi , S.R. Mirghaderi , A. Hosseini & M.E. Shemshadian
Faculty of Civil Engineering, University of Tehran

15 WCEE
LISBOA 2012

SUMMARY:
Buckling restrained braced frames (BRBFs) have been used as seismic load resisting system in recent years. Due to their more effective performance, BRBs have been employed to replace conventional braces in concentrically bracing frames. When compared to conventional braces, BRBs exhibit symmetric and more stable hysteretic behaviour that provide significant energy dissipation capacity and ductility. Since the manufacturing process of the BRBs is expensive and time consuming, and requires considering tight erection tolerances, they have not been commercialized as the common bracing systems in some parts of the world. In order to reach a simpler detailing, all-steel BRB with the idea of eliminating mortar have been proposed and developed in the last years. In the present paper, an innovative all-steel BRB with reduced yielding segment is proposed. In the proposed BRB, the yielding part is located at one end of the brace and steel plates are intended to act as the buckling restraining part. Analytical model is developed using a finite element software and a nonlinear cyclic analysis is performed as per the recommended loading protocol. The results show the steel plates can successfully restrain the buckling of yielding segment of BRB and thus cause the stable and symmetric hysteresis behaviour of the brace.

Keywords: BRB, Abaqus, Low-Cycle Fatigue, Reduced Length BRB, Short Length BRB,Nonlinear Cyclic Analysis

1. INTRODUCTION

Buckling restrained braces (BRBs) have been widely used in seismic design of structures in recent years. BRBF has both high stiffness and ductility in comparison to other lateral resisting systems. In order to reach an optimum seismic design in which most of the energy dissipating potential is utilized, different elements with different strength and stiffness are required. The stiffness and strength of a BRB can be tuned independently by selecting different ranges of cross sections and lengths.

Most of the BRB members developed up to now are designed to extend through the full length between two beam to column joints. The ratio of yielding core to the total length (L_c/L) of common BRBs varies from 0.5 to 0.8 in different detailing. Limited studies have been performed on BRBs with small yielding segments with L_c/L of 0.2 to 0.4 (Razavi et al., 2011, Shemshadian et al., 2011b, Ma et al., 2008, Di Sarno and Manfredi, 2009, Ahlehagh, 2008, Tremblay et al., 2006). Besides eliminating concrete, reducing the length of BRB incorporates advantages such as simple replaceability, lesser weight, and easy erection process. Moreover, a small and light BRB is more economical than a normal or heavy BRB. The typical application of reduced length BRB (RLBRB) is depicted in Fig. 1.

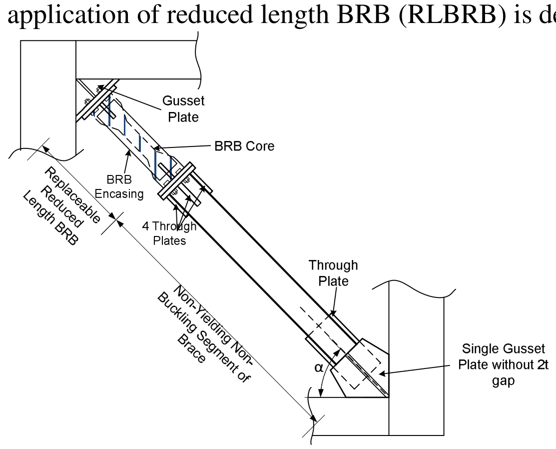

Figure 1. Reduced length BRB in a frame

The strain level in conventional BRBs is usually limited to 1% to 2% (Razavi et al., 2011). By decreasing the core length the plastic strains which is inversely dependant on the yielding length increases. This might arise concerns about low-cycle fatigue (LCF) failure. However, BRBs with higher strains have also shown satisfactory performance. Table 1 lists a number of experimental studies with strain amplitudes larger than 2%.

Table 1. Researches incorporating high strain amplitudes (Bolduc and Tremblay, 2003, Tsai et al., 2004, Tremblay et al., 2006, Mirghaderi and Ahlehagh, 2008, Ma et al., 2008, Mazzolani, 2008, Di Sarno and Manfredi, 2010, Lin et al., 2011)

Researcher	Year	Method of Research	L_c/L	ε_{max}
Tsai et al	2002	Experimental	20%-35%	4-6%
Bloduc and Tremblay	2003	Experimental	17%	3.7%
Tremblay et al	2006	Experimental	25%	3.4%
Mirghaderi and Ahlehagh	2008	Analytical	35%	4.3%
Ma et al	2008	Experimental	20%	3.4%
Mazzolani et al	2008	Experimental	40%	3.5%
Di Sarno and Manfredi	2010	Analytical	30%	3-5%
Lin et al	2011	Experimental	70%	4%

In this study, a detailing for an all-steel reduced length BRB (RLBRB) is presented. The provisions considered in designing and developing the RLBRB are described. Finite element analysis of a tested short BRB is performed to gain insights about modelling assumptions and approaches. Based on the findings of verification modelling, the performance of RLBRB is evaluated by conducting finite element analysis. The results of the analysis are discussed.

2. PRESENTATION OF REDUCED LENGTH BRB

As noted before, reducing the length of yielding part and encasing member can bring forth improvements to BRB. Since the friction force between the core and encasing is a function of the contact points and total length and higher mode buckling wavelength is constant for same steels and cross sections, a BRB with lesser length would probably develop lesser friction force. Less residual drifts and better seismic performance are other advantages of reducing the yielding lengths in BRB frames (Razavi et al., 2011, Shemshadian et al., 2011b, Alireza Mehdipanah et al., 2012).

In the proposed system, the BRB yields in tension and compression and the rest of the brace is designed to remain elastic (Fig. 1). In other words, the BRB acts as the displacement controlled component and the rest of the brace acts as the force controlled component. The design procedure of such a system is thoroughly described by Razavi et al (Razavi et al., 2011).

2.1. Position of Core in Reduced Length BRB

As shown in Fig. 2(a), in most of normal BRBs the encasing is placed on the whole BRB except the gusset plate, connections. In some limited researches (Ma et al., 2008, Tremblay et al., 2006) the encasing length has been reduced and placed on a portion of the brace in the middle (Fig 2(b)).

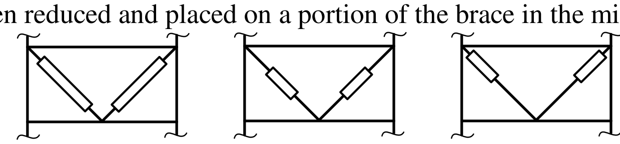

(a) (b) (c)

Figure 2. Normal length and reduced length BRBs with different core positions

Reducing the encasing length makes the total brace susceptible to global buckling. So controlling the global buckling of the brace is one of the design criteria of the RLBRB. Mirghaderi and Ahlehagh studied the buckling load of an axial member with a weak section in a limited length of it (Mirghaderi and Ahlehagh, 2008). The results of this study shows that as the weak section gets close to one end of the member the buckling load of the member increases. In other words, the least buckling load is for the case where the weak section is in the middle and the maximum buckling load is gained when the weak section is placed at one end of brace (Fig. 3(a)).

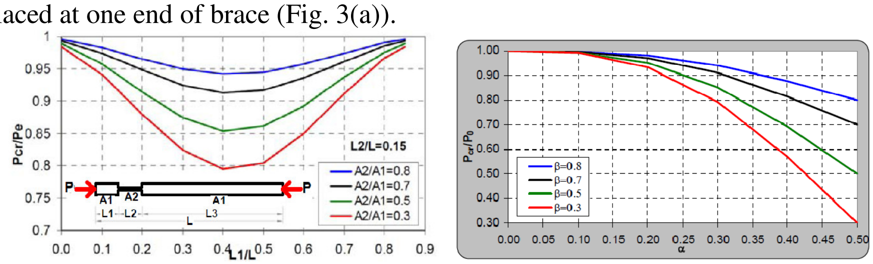

(a) with the change in position of weak section (b) with the change in length of weak section

Figure 3. Change in critical buckling load (Mirghaderi and Ahlehagh, 2008)

Fig. 3(b) shows change in buckling load for different lengths of weak section (α and β are the ratio of weak section length and area to that of brace respectively). As expected, when the length of weak section increases, the critical buckling load decreases. Preventing the global buckling is the main criteria for designing the brace in RLBRB; so by selecting lesser length and positioning the core at one end of the brace, minimum decrease in critical buckling load of brace is gained which is the most economic case. From the practical point of view, guiding the position of reduced length BRB to the ends of the brace makes the BRB fuse more replaceable and provides application of X pattern in BRBFs. Thus; in developing the idea of RLBRB; the yielding section is shifted to brace end (Fig. 1 and Fig. 2(c)) and the core length is minimized to the extent LCF failure is prevented.

2.2. Low-Cycle Fatigue

The reduction in BRB core length and consequently the increase in strain of core to amplitudes of 4-5% increases the risk of low-cycle fatigue failure. From the metallurgical point of view the fatigue life is evaluated by Coffin-Manson equation based on small axial tests (Stephens et al., 2000). The state of strain in BRB core is affected by axial actions as well as in-plane and out of plain actions. However, Coffin-Manson equations for different BRBs especially with high amplitude strains or small yielding lengths are developed by many researchers. Table 2 lists a number of Coffin-Manson equations developed for BRB with steel core.

Table 2. Some Coffin-Manson equations developed for BRB (Nakamura et al., 2000, Koetaka et al., 2001, ISODA et al., 2002, NARIHARA et al., 2002, HORIE et al., 2003, KAMURA et al., 2009, Usami et al., 2011a)

Researcher	Year	Location	Equation	Steel Grade	Test Type
Nakamura et al	2000	Japan	$\Delta\varepsilon=0.2048N_f^{-0.490}$	SN400B	Uniaxial
				LYP100	
				LYP235	
Koetaka et al	2001	Japan	$\Delta\varepsilon=0.0918N_f^{-0.394}$	LYP100	Sub-assemblage
				LYP235	
Isoda et al	2002	Japan	$\Delta\varepsilon=0.20N_f^{-0.39}$	LY225	Uniaxial
Nariharah	2002	Japan	$\Delta\varepsilon=0.3771N_f^{-0.602}$	SN400B	Sub-assemblage
Horie et al	2003	Japan	$\Delta\varepsilon=0.20N_f^{-0.41}$	SNB400	Uniaxial
Kamura et al	2009	Japan	$\Delta\varepsilon=0.1128N_f^{-0.4129}$	LY100	Uniaxial
Usami (As-Welded)	2011	Japan	$\Delta\varepsilon=0.210N_f^{-0.488}$	SM400A	Uniaxial
Usami (Toe-finishing)	2011	Japan	$\Delta\varepsilon=0.171N_f^{-0.401}$		

Generally LCF capacity depends on various factors such as shape of core segment, stiffness of buckling restraining mechanism, width to thickness ratio of the axial member, core-encasing gap, friction between core and restraining mechanism, eccentricity in the core segment, overall detailing of the BRB, and the quality of manufacturing. Moreover, the overall fatigue life of BRBs is somehow similar for different steel grades. The results of LCF test (Usami et al., 2011a, Usami et al., 2011b) show that presence of any discontinuities, geometric changes, tack welds, attachments in core segment which is identified as protected zone in AISC 341-10 (AISC, 2010), severely degrades the LCF life. LCF failure occurs soon after the formation of local buckling in the core segment (Shemshadian et al., 2011a). Using sections other than flat plates like cruciform sections decreases the fatigue life property (Nakamura et al., 2000, Iwata et al., 2012). Attention is paid to these findings in developing the detailing of the RLBRB.

In order to prevent LCF failure, the Palmgren-Miner rule is controlled for two standard loading protocols (Miner, 1945). AISC 341-10 (AISC, 2010) specifies a loading protocol for testing BRBs. Moreover ASCE 7-10 (ASCE07-10, 2010) defines the sequence and cycles of testing for seismic energy damping devices. The AISC 341-10 loading protocol is developed for BRBF structures located along the west coast of California and designed according to the USA provisions (Sabelli et al., 2003). Dehghani and Tremblay conducted a large number of nonlinear time history analyses by selecting a set of 20 seismic records on 56 multi-storey BRBFs and showed that this loading protocol overestimates the demands on BRBs (Dehghani and Tremblay, 2012). The inherent post-elastic stiffness of the systems equipped with RLBRB hardly allows the story to experience design drifts up to 1.5%. In this study, the loading protocol recommended by FEMA 450 (BSSC, 2003) with the maximum drift of 1.5 Δ_{bm} was selected. AISC 341-10 and OSHPD regulations (Merritt et al., 2003) require cumulative inelastic axial deformation (η) of at least 200 and 350 times the yield deformation respectively to be considered in developing the loading protocol.

In Fig. 4 a number of Coffin-Manson curves for some previously tested specimens are shown. This figure indicates that the equation developed by Nakamura et al (Nakamura et al., 2000) corporate enough conservativeness for evaluating BRB fatigue capacity.

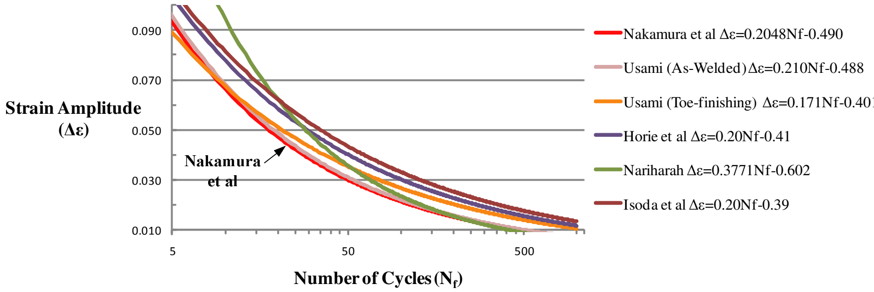

Figure 4. Coffin Manson Equations developed based on experimental results

Using this equation and assuming a design story drift of 1.5%, the minimum required length for calculating strain demand on the brace for a typical 3 m high, 5 m width bay with chevron pattern to prevent LCF to the end of FEMA-450 loading protocol with η of 370 will be 110 cm. The displacement controlled loading protocol for RLBRB is shown in Fig. 5.

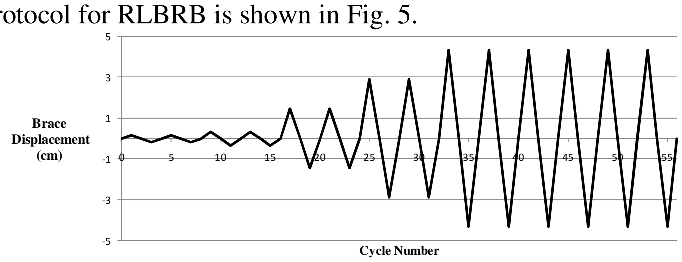

Figure 5. Loading Protocol

Assuming the story drift at MCE level to be 1.5 times the design story drift, the BRB with this length is capable of withstanding 7 full cycles at MCE earthquake which well satisfies the ASCE 07-10 provision for damping devices. The details of calculating the required length of BRB is described by Razavi et al (Razavi et al., 2011).

2.3. Energy Dissipating Capacity

Reducing the BRB length causes the energy dissipation to be locally concentrated in a limited length of the brace. Although the volume of steel material participating in energy dissipation through plastic strains decreases, the energy dissipation capacity of the brace is not affected. This fact can be verified by calculating the area of a stress-strain hysteresis loop developed based on kinematic hardening rule.

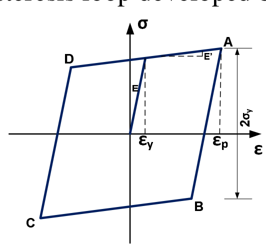

Figure 6. Stress strain hysteresis loop for BRB

Using the polygon formula for calculating area of parallelogram based on point coordinates, the density of dissipating energy would be reduced to:

$$E(\varepsilon) = \frac{4\sigma_y}{E}(E - E')(\varepsilon_p - \varepsilon_y) \tag{1}$$

where σ_y and ε_y are the yield stress and strain, E and E' are the elastic and plastic modulus, and ε_p is the core plastic strain corresponding to the story drift. By assuming a uniform strain distribution through the length of core, the energy dissipated by an element within a complete cycle is calculated by multiplying the energy density by area and length of the member:

$$E(\Delta) = \frac{4F_y}{E}(E - E')(\Delta_p - \Delta_y) \tag{2}$$

where F_y and Δ_y are brace yield force and displacements, and Δ_p is brace displacement corresponding to the story drift. Equation 2 shows that at same story drifts, energy dissipated by BRBs with same steel grades and cross section areas is not dependant on the length. Nevertheless, if the isotropic hardening is to be taken into account, the friction force between the core and encasing makes the judgment about energy dissipation capacity somehow difficult. The reason is that by the decrease in length, the frictional force and isotropic behavior reduces, but the strain levels and local buckling are intensified. In an experimental study, Mirtaheri et al showed that as the BRB length decreases the energy dissipation capacity increases (Mirtaheri et al., 2011).

2.4. Detailing and Design Provisions of RLBRB

The core of RLBRB is a 80×10 mm plate made of ST 37 (DIN) steel. The encasing is a 180×10 mm ST 37 plate reinforced by a rectangular HSS 60×60×5 for out of plane action. The encasing is designed to well satisfy the Watanabe criteria (Watanabe et al., 1988) to have proper action in high axial displacements. The two encasings are connected through two 50×14 filler plates with high strength European grade 8.8 bolts (BS, 2001) 10 mm in diameter spaced 5 cm centre to centre. Using bolts helps to disassemble the specimen after test and closely investigate the core performance. Furthermore the encasing and fillers can be used more than one time for experimental purposes. The end of core is stiffened by two trapezoidal 20×80×10 plates. The load is transferred to the core from two 300×300×30 end plates. CJP groove welds connect the core and stiffeners to the end plates. End plates are connected to adjacent connection with 8 high strength European grade 8.8 bolts (BS, 2001) 22 mm in diameter. A 1 mm gap through thickness and 3 mm gap through width of core plate is considered for allowing expansion in compression cycles in each side. The 1 mm gap is provided by wrapping pipe wrap tape. Fig. 7 shows 3D view and section of RLBRB.

One of the crucial criterions governing the design of the proposed BRB is preventing LCF failure. Any stress or strain concentration can trigger LCF failure. The assumption for gaining a proper length for the BRB is based on uniform distribution of axial strain through the length of yielding part. The previous studies show that due to the presence of friction force between the core and encasing, this assumption is not valid (Korzekwa and Tremblay, 2009, Eryasar and Topkaya, 2009, Tremblay et al., 2006).

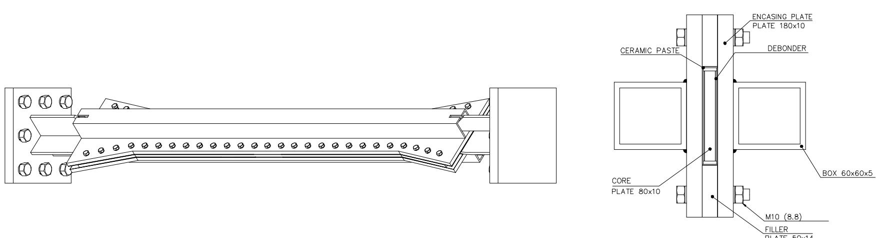

Figure 7. 3D view and section of RLBRB

One of the main reasons for non-uniform strain distribution is the initiation of frictional contact between the core and encasing, especially at both ends which are the first points that experience local buckling. This will cause the inner parts of the core experience lesser compressive force than the end parts . On the contrary, the two ends have less participation in carrying the tensile load than the middle core which causes necking of this part in higher strains. In order to develop a BRB with the least potential to LCF failure, the friction between the core and encasing should be the least possible amount. Therefore, unlike some other types of BRB in which no debonder has been used (Chou and Chen, 2010), applying the debonder is one of the necessities of the proposed BRB. Ceramic has shown minimal friction to steel, especially when covered with grease (Andersson and Ylöstalo, 1989). Hosseini and Ansari used a kind of ceramic paste on core element in order to decrease the steel to concrete friction (Ansari, 2010). Although the paste could successfully reduce the friction between steel surfaces, it crushed at large compression cycles due to local buckling of the core. In the proposed BRB, the ceramic paste is painted on the encasing which remains elastic and experiences little deformation.

The encasing is responsible for preventing global buckling of the core as well as limiting local bucklings. In order to fix the encasing on the core, several detailings have been proposed up to now. Friction can help the encasing to hold the core; however, since the friction is not favorable in BRB design procedure and the relative movement of the core to encasing is not predictable, this method cannot be trustable (Eryasar, 2009, Ansari, 2010). A steel stopper pin has been placed on one point of the flat face of the core to connect the encasing to the core (Iwata et al., 2012, Usami et al., 2005, Nakamura et al., 2000). An outward projection of the core in the middle length formed by CNC cut or tack welds has been utilized in some other schemes (Chou and Chen, 2010, Eryasar and Topkaya, 2009, Lin and Tsai, 2003). Slotted holes in core plate at end regions of the brace were provided by Tremblay et al to keep the steel encasings on the core. (Tremblay et al., 2006)

AISC seismic provision (AISC, 2010) introduces the core plate as the protected zone on which no attachments are permitted. The best place to fix the encasing to core is the middle of core. Because the two end distances of encasing to end plates will be equal and the lateral gap between encasing and the core is half of the condition encasing is connected to core at one end. In order to omit any discontinuity in the core plate, in the proposed detailing a copper plate has been placed on the core in the middle length. The thin copper plate with half of steel modulus of elasticity and high friction with steel fills the gap between the core and encasing, and when pressured by snug-tight bolts, initiates a local favorable friction. By following this approach the AISC criteria for protected zone of core is satisfied. Fig. 8 shows the detailing of placing copper plate on core plate. In order to prevent stress concentration on the core, the width of core section is gradually increased so that it reduces the stress from failure strength (F_u) to 0.9 F_y at end stiffeners (Fig. 8).

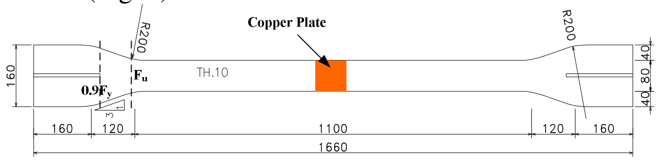

Figure 8. Plan of BRB core with copper plate

3. MODELING AND FINITE ELEMENT MODEL OF A TESTED BRB

In order to verify the analytical results of RLBRB, finite element model of a specimen tested by Eryasar and Topkaya (Eryasar, 2009) was analysed using ABAQUS 6.10 (Abaqus, 2010). This study was selected by the authors since there are similarities between the concepts of proposed BRB and the specimens tested by Eryasar and Topkaya.

3.1. Description of Tested BRB

Eryasar and Topkaya have tested 12 down scaled all-steel BRB under a uniaxial test setup with 250 kN screw jack. In the first 6 set of BRBs, the effect of bolt spacing and pretension and welding condition was studied. Moreover, the core to encasing connection was investigated in the first set. The encasing member is composed of standard available steel channels. In the second 6 BRBs they tried to provide an efficient encasing detailing. The core was connected to the encasing by depositing a tack weld on the middle length of the core. In all specimens, the core was wrapped by 4 layers of 0.05 mm polyethylene film permitting a 0.2 mm gap through thickness. A gap of 1 mm was considered through width in each side. In the present study specimen 11 is selected for verification purposes. The detailing of this specimen is shown in Fig. 9. The core plate material was made of European S275 grade (CEN, 1994) steel and with the yield stress (F_y) and ultimate stress (F_u) was 280 MPa and 420 MPa respectively. The strain demand at the design level is taken as 1 percent (Eryasar, 2009).

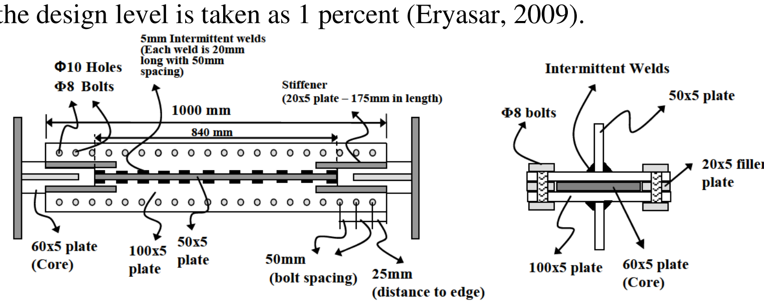

Figure 9. Detailing of specimen 11 (Eryasar, 2009)

3.2. Finite Element Modelling of Specimen 11

The finite element model of the specimen 11 is carried out using ABAQUS 6.10 (Abaqus, 2010). As shown in Fig. 10 the model includes the core plate, filler plates, the encasing members and the end stiffeners. The axial stiffness of the bolts are high, so the bolt point are considered constraint with the fillers and encasings. All the plates were modelled using C3D8 solid elements. A finer mesh is adopted for the core plate with 7 elements across the core plate and 2 over the thickness. The model includes a total of 8064 elements (1788 for the core). The contact properties considering both normal behaviour without penetration and tangential actions are defined on 4 surfaces of the core plate and other related surfaces. Due to the use of grease between steel and polyethylene film, the friction coefficient of 0.075 is selected. The encasing is tie constrained to the core at its centre.

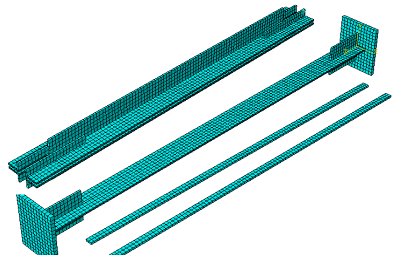

Figure 10. Finite element model of specimen 11

Mixed plasticity including kinematic and isotropic hardening is used for steel core material. Two backstresses was considered to more accurately capture kinematic hardening. Initial 0.2 mm and 1 mm gaps are left between the core and encasing for the in-plane and out of plane direction of core section. A half-gap out of plate imperfection is imposed at both two ends and the middle of the core in opposite directions. The loading protocol used for the test is applied to the end plate. The analysis took 6 hours on a personal computer with CORE i5 intel CPU and 8 Gb RAM.

3.3. Results

Fig. 11 shows the finite element analysis curve and the data obtained from test for specimen 11. In this curve tension force is depicted in positive side of vertical axis. Generally the force-displacement curve is in good agreement with the experimental data. The elastic and post elastic stiffness of the model is almost the same as the test. The maximum force in tension and compression is well predicted. The ratio of compression force to tensile force is computed 5.3% in the analytical model which is well comparable to that of the test.

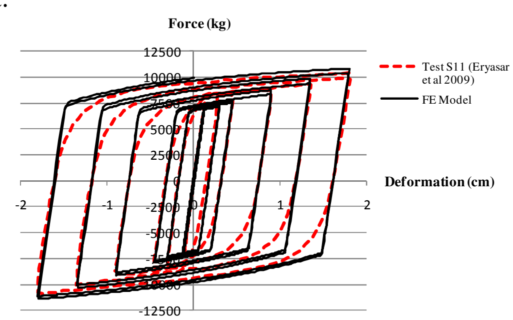

Figure 11. Finite element analysis and test results for specimen 11

The analysis has successfully captured both contact between core and encasing plates and local buckling of the core in compressive cycles. Fig. 12(b) shows the out of plane buckling of the core in the final compressive cycle (2 Δ_{bm}) corresponding to strain of 2%, which is comparable to that of test (Fig. 12(a)). The stress concentration can be easily seen in Fig. 12(c) where no transition detailing is considered in the design of this kind of BRB. Based on the similarities between specimen 11 and the RLBRB, the basic modeling assumption and approaches of this section could be reasonably valid for using in modeling of RLBRB.

(a) Local buckling of tested core at strain of 2%

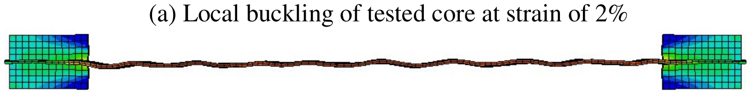

(b) Local buckling of model of core at strain of 2%

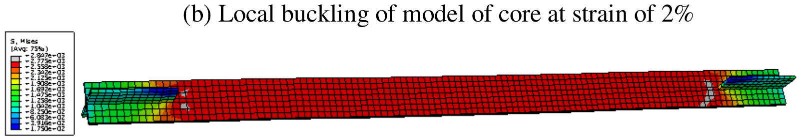

(c) Deformed shape and Von Mises stress of specimen 11 at maximum displacement

Figure 12. Deformation and stress state of specimen 11

4. FINITE ELEMENT ANALYSIS AND RESULTS OF THE PROPOSED BRB

Based on the modeling assumptions adopted in the previous section, the performance of the proposed BRB is evaluated by conducting nonlinear finite element analysis.

4.1. Finite Element Modelling of Proposed BRB

The model includes the core plate, copper plates, filler plates, the encasing members (plate and box), end stiffeners, and end plates. The same approach as the previous section for the bolts was followed. A C3D8 solid element has been used to model all parts. The core plate is divided into 6 elements across the width and 2 over the thickness. The model includes a total of 7124 elements (1743 for the core). The finite element model of the proposed BRB is shown in Fig. 13.

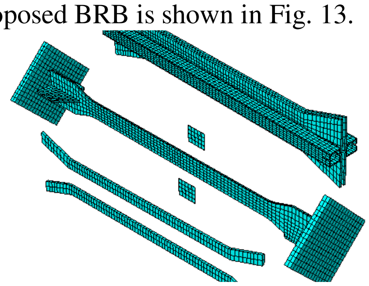

Figure 13. Finite element model of proposed BRB

The same contact properties as in previous section are considered. A frictional coefficient of 0.05 was adopted to simulate greasy steel to ceramic interfaces. The encasing is constrained to the core at copper plate location. The core and encasing plates were made of ST 37 (DIN17100) with nominal yield strength (F_y) of 2400 kg/cm^2 and rupture strength (F_u) of 3700 kg/cm^2. The coupon tests (ASTM, 2002) resulted F_y=2500 kg/cm^2 and F_u= 4100 kg/cm^2. Other steel part which remain elastic are assigned the same steel material properties. Initial 1 mm and 3 mm gaps were left between the core and encasing in the in plane and out of plane direction of core section for allowing lateral expansion due to Poisson effect. A half-gap out of plate imperfection was imposed at both two ends in a state with no rotational stiffness for end plates. For convergence purpose automatic stabilization with a damping factor of 2E-7 was used. The loading protocol shown in Fig. 5 was applied to the end plate. The analysis took 7 hours on a personal computer with CORE i5 intel CPU and 8 Gb RAM. The energy dissipated for stabilization purpose is minimal and does not affect the results.

4.2. Results and Discussion

The force-deformation curve obtained from the finite element analysis of RLBRB is shown in Fig. 14. The maximum difference between compression force and tension force is 11%, which is below the permissible limit noted in AISC 341-10. The analysis results cannot be trusted due to excessive necking in the core in the beginning of cycles corresponding to 1.5 Δ_{bm}. Necking is the result of friction initiated between the core and encasing at ends of the core. The preliminary analysis showed that initial imperfection, element type, and friction coefficient are effective in the onset of necking.

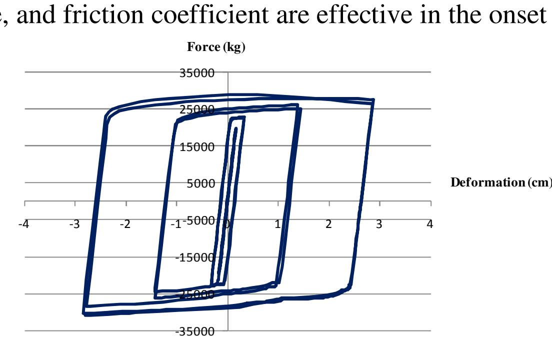

Figure 14. Finite element analysis result for RLBRB

Although a lesser friction coefficient was applied, the friction force initiated between surfaces is higher than specimen 11. The reason for this fact is higher strains experienced by RLBRB. Fig. 15 shows the Von Mises stress state in the core at the maximum compressive displacement. The transition zone designed for the proposed BRB has well guaranteed the elastic state of core.

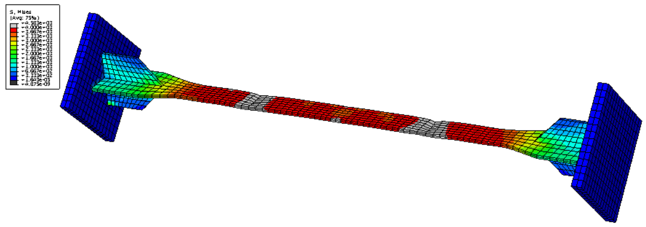

Figure 15. Deformed shape and Von Mises stress of RLBRB at maximum compressive displacement

The final stage of analysis show that although the displacement has come to zero, the local buckling are still present in the core which is in agreement the finding of past experimental studies (Tremblay et al., 2006).

The bolt spacing is proper for controlling the local buckling. The encasing has remained elastic till the end of analysis. Fig. 16 shows deformed shape of encasing and the normal contact forces exerted on it.

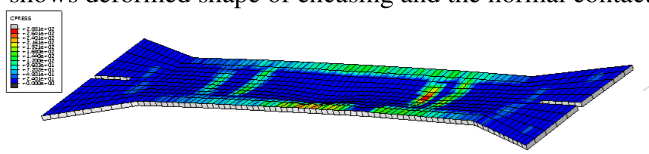

Figure 16. Deformed shape and normal contact force on encasing at maximum compressive displacement

5. CONCLUSIONS

In this study, the advantages of reducing the BRB length were discussed. A type of all-steel reduced length BRB (RLBRB) was presented and the design provisions as well as detailing considerations were expanded. A finite element analysis was performed on a previously tested BRB to gain proper insight for modelling attempts. The performance of RLBRB was evaluated by finite element analysis. The results of the analysis show that the proposed BRB can satisfy the requirements of AISC 341-10 for buckling restrained braces. The hysteresis loop is stable up to strains corresponding to design drifts and no degradation occurs in the curve. The encasing and bolt spacing are enough to guarantee the performance of BRB core to the end of analysis.

The results of this study show that simpler BRB systems with less practical and economical efforts can be developed in places where BRB systems have not been developed and even in other places. It is noteworthy that the obtained results should be verified by the experimental evidences which are to be performed by the authors in the near future.

REFERENCES

ABAQUS. (2010). Abaqus, Users' Manual. Karlsson, and Sorensen, Inc., Providence, RI.

AHLEHAGH, S. (2008). *Improvement of the Special Concentrically Braced Steel Frames Behavior by Employing Balanced Braces.* Master of Science, University of Tehran.

ANSI/AISC 341-10. (2010). Seismic Provisions for Structural Steel Buildings. AISC. Chicago, Illinois.

ALIREZA MEHDIPANAH, A., MIRGHADERI, S. R. & RAZAVI, S. A. (2012). Seismic Assessment of Buckling Restrained Braced Frame Dual System with Special Moment Resisting Frame. *Proceedings of the 4th International Conference on Seismic Retrofitting*.

ANDERSSON, P. & YLÖSTALO, O. (1989). The influence of lubrication on ceramic and steel sliding contacts. *Materials Science and Engineering: A,* **109,** 407-413.

ANSARI, M. (2010). *Numerical and Experimental Study of Buckling Restrained Braces.* Master of Science in Civil Engineering, Uinversity of Tehran.

ASCE07-10. (2010). Minimum Design Loads for Buildings and Other Structures. American Society of Civil Engineers

ASTM A270. (2002). Standard Test Methods and Definitions for Mechanical Testing of Steel Products. ASTM.

BOLDUC, P. & TREMBLAY, R. (2003). Experimental Study of the Seismic Behaviour of Steel Braces with Concrete Filled Tube and Double Steel Tube Buckling Restrained Mechanisms. CGM Department, Ecole Polytechnique.

BS. (2001). Specification for Iso-Metric Precision Hexagon Bolts, Scres and Nuts. *BS 3692.* London.

BSSC. (2003). NEHRP recommended provisions for seismic regulations for new buildings and other structures (FEMA 450). *National Earthquake Hazards Reduction Program.* Building Seismic Safety Council, Federal Emergency Management Agency.

EN 10025. (1994). Hot rolled products of non-alloy structural steel. CEN. Brussels.

CHOU, C. C. & CHEN, S. Y. (2010). Subassemblage tests and finite element analyses of sandwiched buckling-restrained braces. *Engineering Structures,* **32,** 2108-2121.

DEHGHANI, M. & TREMBLAY, R. (2012). Development of standard dynamic loading protocol for buckling-restrained braced frames. *International Specialty Conference on Behaviour of Steel Structures in Seismic Area (STESSA).*

DI SARNO, L. & MANFREDI, G. (2009). Numerical simulation of the cyclic inelastic behaviour of buckling restrained braces. *ATC & SEI 2009 Conference on Improving the Seismic Performance of Existing Buildings and Other Structures*.

DI SARNO, L. & MANFREDI, G. (2010). Seismic retrofitting with buckling restrained braces: Application to an existing non-ductile RC framed building. *Soil Dynamics and Earthquake Engineering*.

STEEL FOR GENERAL STRUCTURAL PUROSES. DIN17100. Germany.

DIN 17100. STEEL FOR GENERAL STRUCTURAL PUROSES. DIN. Germany.

ERYASAR, M. E. (2009). *EXPERIMENTAL AND NUMERICAL INVESTIGATION OF BUCKLING RESTRAINED BRACES.* MASTER OF SCIENCE IN CIVIL ENGINEERING, MIDDLE EAST TECHNICAL UNIVERSITY.

ERYASAR, M. E. & TOPKAYA, C. (2009). An experimental study on steel-encased buckling-restrained brace hysteretic dampers. *Earthquake Engineering & Structural Dynamics*.

HORIE, T., MASE, S. & TERADA, T. (2003). Development of Unbonded Brace Damper Restrained by Channel Section Steel. Part 5 Low Cycle Fatigue Tests on Unbonded Brace Dampers with SN400B. Architectural Institute of Japan.

ISODA, K., SATAKE, N., MASE, S., TERADA, T. & HORIE, T. (2002). Development of Unbonded Brace Damper Restrained by Channel Section Steel. Part.4 Low Cyc1e Fatigue Tests. Architectural Institute of Japan.

IWATA, M., MURAIM, M. & NAKAGOMI, T. (2012). Experimental study on brittle fracture of buckling-restrained braces influences of core plate welding specifications and experimental temperatures. *International Specialty Conference on Behaviour of Steel Structures in Seismic Area (STESSA).*

KAMURA, H., NANBA, T., OKI, K. & FUNABA, T. (2009). Seismic Response Control for High-Rise Buildings Using Energy-Dissipation Devices, JFE TECHNICAL REPORT.

KOETAKA, Y., NARIHARA, H. & TSUJITA, O. (2001). Part 3 Low Cycle Fatigue Test on Aseismic Braces. The Experimental Study on Buckling Restrained Braces Architectural Institute of Japan.

KORZEKWA, A. & TREMBLAY, R. (2009). Numerical simulation of the cyclic inelastic behaviour of buckling restrained braces. *International Specialty Conference on Behaviour of Steel Structures in Seismic Area (STESSA).*

LIN, P. C., TSAI, K. C., WANG, K. J., YU, Y. J., WEI, C. Y., WU, A. C., TSAI, C. Y., LIN, C. H., CHEN, J. C. & SCHELLENBERG, A. H. (2011). Seismic design and hybrid tests of a full-scale three-story buckling-restrained braced frame using welded end connections and thin profile. *Earthquake Engineering & Structural Dynamics*.

LIN, S. L. & TSAI, K. C. (2003). A Study of All Metallic and Detachable Buckling Braces. Center for Earthquake Engineering Research, National Taiwan University.

MA, N., WU, B., LI, H., OU, J. & YANG, W. (2008). Full Scale Test of All-Steel Buckling Restrained Braces. *14th World Conference on Earthquake Engineering.* Beijing, China.

MAZZOLANI, F. (2008). Innovative metal systems for seismic upgrading of RC structures. *Journal of Constructional Steel Research,* **64,** 882-895.

MERRITT, S., UANG, C.-M. & BENZONI, G. (2003). SUBASSEMBLAGE TESTING OF STAR SEISMIC BUCKLING-RESTRAINED BRACES. Pacific Earthquake Engineering Research Center, University of California at Berkeley. UNIVERSITY OF CALIFORNIA, S. D.

MINER, M. (1945). Cumulative damage in fatigue. *Journal of Applied Mechanics*.

MIRGHADERI, R. & AHLEHAGH, S. (2008). STUDY OF SEISMIC BEHAVIOR OF SCBF WITH "BALANCED BRACING". *14th World Conference on Earthquake Engineering*.

MIRTAHERI, M., GHEIDI, A., ZANDI, A. P., ALANJARI, P. & SAMANI, H. R. (2011). Experimental optimization studies on steel core lengths in buckling restrained braces. *Journal of Constructional Steel Research*.

NAKAMURA, H., MAEDA, Y. & SASAKI, T. (2000). Fatigue Properties of Practical-Scale Unbonded Braces. Nippon Steel.

NARIHARA, H., TSUJLTA, O. & S., Y. (2002). The Experimental Study on Buckling Restrained Braces. Part 4 Low Cycle Fatigue Test on Aseismic Brace with SN400B, SN490B. Architectural Institute of Japan.

RAZAVI, S. A., SHEMSHADIAN, M. E., MIRGHADERI, S. R. & AHLEHAGH, S. (2011). Seismic design of buckling restrained braced frames with reduced core length. *The Structural Engineers World Congress* Italy.

SABELLI, R., MAHIN, S. & CHANG, C. (2003). Seismic demands on steel braced frame buildings with buckling-restrained braces. *Journal of Engineering Structures,* **25,** 655-666.

SHEMSHADIAN, M. E., RAZAVI, S. A., HOSSEINI, A., MIRGHADERI, S. R. & KHAN MOHAMMADI, M. (2011a). An Analytical Study on Low Cycle Fatigue Effects in Buckling Restrained Braces. *Computational Methods in Structural Dynamics and Earthquake Engineering.* Corfu, Greece.

SHEMSHADIAN, M. E., RAZAVI, S. A., MIRGHADERI, S. R., HOSSEINI, A. & KHAN MOHAMMADI, M. (2011b). The Advantages of Reducing the Length of Yielding Segment in Seismic Performance of Buckling Restrained Braced Frames. *Sixth International Conference of Seismology and Earthquake Engineering.* Tehran, Iran.

STEPHENS, R., FUCHS, H., FATEMI, A. & STEPHENS, R. (2000). Metal Fatigue in Engineering, Wiley-Interscience.

TREMBLAY, R., BOLDUC, P., NEVILLE, R. & DEVALL, R. (2006). Seismic testing and performance of buckling-restrained bracing systems. *Canadian Journal of Civil Engineering,* **33,** 183-198.

TSAI, K. Q., LAI, J.-W., HWANG, Y.-C., LIN, S.-L. & WENG, C.-H. (2004). RESEARCH AND APPLICATIONS OF DOUBLE-CORED BUCKLING RESTRAINED BRACES. *13th World Conference on Earthquake Engineering.* Vancouver, B.C., Canada.

USAMI, T., LU, Z. & GE, H. (2005). A seismic upgrading method for steel arch bridges using buckling restrained braces. *Earthquake engineering & structural dynamics,* **34,** 471-496.

USAMI, T., WANG, C. & FUNAYAMA, J. (2011a). Low-Cycle Fatigue Tests of a Type of Buckling Restrained Braces. *Procedia Engineering,* **14 (2011)** 956–964.

USAMI, T., WANG, C. L. & FUNAYAMA, J. (2011b). Developing high-performance aluminum alloy buckling-restrained braces based on series of low-cycle fatigue tests. *Earthquake Engineering & Structural Dynamics*.

WATANABE, A., HITOMI, Y., YAEKI, E., WADA, A. & FUJIMOTO, M. (1988). Properties of brace encased in buckling-restraining concrete and steel tube. *9th World Conference on Earthquake Engineering.* Tokyo-Kyoto, Japan.